İSTANBUL UNIVERSITY CERRAHPAŞA

ORIGINAL ARTICLE
Electrica 2025; 25: 1-14

Performance Comparison of Different PV Array Configurations Considering the Number of Bypass Diodes Under Partial Shading

Hatice Gül Sezgin-Ugranlı

Department of Electrical-Electronics Engineering, İzmir Bakırçay University Faculty of Engineering and Architecture, İzmir, Türkiye

Cite this article as: H. G. Sezgin-Ugranlı, "Performance comparison of different PV array configurations considering the number of bypass diodes under partial shading," *Electrica*. 2025, 25, 0080 doi: 10.5152/electrica.2025.25080.

WHAT IS ALREADY KNOWN ON THIS TOPIC?

- *Partial shading significantly reduces photovoltaic system performance by causing mismatch losses that are conventionally mitigated using bypass diodes and appropriate array configurations.*

WHAT THIS STUDY ADDS ON THIS TOPIC?

- *While previous research has explored the general impact of bypass diodes, the specific effect of the number of bypass diodes across different array topologies remains an open question.*
- *Comparisons of array configurations would be more appropriate to conduct site-specific evaluations that account for both the number of bypass diodes and the severity of partial shading condition.*

Corresponding Author:
Hatice Gül Sezgin-Ugranlı

E-mail:
haticegul.ugranli@bakircay.edu.tr

Received: April 11, 2025
Revision requested: July 4, 2025
Last revision received: July 15, 2025
Accepted: July 28, 2025
Publication Date: October 15, 2025

DOI: 10.5152/electrica.2025.25080

ABSTRACT

Partial shading is one of the most critical challenges affecting the performance and reliability of photovoltaic (PV) systems in real-world scenarios. Although bypass diodes are widely used to reduce mismatch losses in PV systems, their role is still under investigation. The effect of increasing their number on overall system performance is especially unclear for different PV array configurations. This study presents a comprehensive simulation-based analysis of how the number of bypass diodes influences the global maximum power point (GMPP) in four widely used PV array configurations: series-parallel, bridge-link, honey-comb, and total cross-tied. A MATLAB Simscape model is employed to simulate 30 shading scenarios. P-V curves are generated in order to determine the current, power, and voltage at GMPP for various bypass diode configurations, with between 6 and 24 cells per bypass diode. In this way, the individual performance of each case across different shading scenarios is compared, and the average values are computed to facilitate a comprehensive comparison of the overall performance among the so-called array configurations. The results not only reveal the relationship between array and bypass diode configurations but also offer new perspectives on how to maximize energy yield in shade-prone PV systems.

***Index Terms*—**Bypass diode, MATLAB Simscape, performance, photovoltaics, photovoltaic (PV) array configuration

I. INTRODUCTION

Solar energy holds a dominant position in the global energy transition as the fastest-growing renewable energy source and provides a significant contribution to reducing dependence on fossil fuels, enhancing the reliability of energy supply, and overcoming the climate crisis [1]. This trend brings an even more critical role for research to achieve operational excellence in photovoltaic (PV) systems in response to the complexities of real-world conditions.

The performance of PV systems is primarily determined by the efficiency of solar cells, which convert sunlight into electrical energy. Since a module is a collection of cells connected in series and/or parallel, the condition of each cell has a major impact on the system's energy flow. Any performance loss in a single cell can reduce the power generation capacity of the other cells in the module, ultimately affecting the entire string [2]. The PV systems often encounter some mismatch challenges due to manufacturer tolerances, partial shading, and dynamic environmental conditions [3]. The mismatch problem is particularly evident under partial shading conditions, where shaded cells limit current flow and significantly reduce overall system performance [4]. Partial shading occurs due to factors such as persistent shading sources (e.g., nearby objects, chimneys, and vegetation), nonuniform soiling (e.g., dust accumulation, bird droppings, and pollution), structural obstructions (e.g., module frames and mounting structures), and seasonal variations in shading patterns [5]. It is particularly unavoidable in building-integrated PV (BIPV) systems due to their exposure to surrounding structures and environmental constraints [6, 7]. Shading not only reduces the power generation capacity of the system but can also trigger reliability problems such as hotspots and ultimately degradation [8]. Even the slightest drop in performance can have a serious impact on profit margins in the long term [9]. Consequently, there is a pressing need for the development of advanced, sensitive, and adaptive methods to improve system performance.

Various techniques have been proposed to mitigate the effects of partial shading on PV systems, including the use of bypass diodes, advanced maximum power point tracking (MPPT) algorithms, module-integrated power electronics, PV array configurations, and reconfiguration methods [10]. Some researchers have focused on developing metrics and parameters to better quantify the shading effects on PV module performance. In line with these efforts, a numerical index based on the differentiation and integration of power-voltage (P-V) curves is developed to detect partial shading, quantify its intensity, and estimate hotspot occurrence time [11]. A bypass diode scanning algorithm for PV arrays is also introduced. It uses bypass diode voltage drop measurements to efficiently track the global maximum power point (GMPP) under partial shading conditions. This leads to higher power extraction, reduced oscillations, and fast response [12]. Additionally, a generalized analytical approach is developed to model the current-voltage (I-V) and power-voltage (P-V) characteristics of PV arrays under partial shading. This method uses standard test conditions (STC) and a two-diode model that incorporates the effects of bypass and blocking diodes in any series-parallel (SP) configuration [13]. In terms of the irradiance profile, mismatch losses caused by partial shading from moving clouds are also analyzed under various irradiance transitions, considering the impact of different electrical configurations on large-scale PV plants [14]. As partial shading introduces multiple local maxima in the P-V curve, locating the global maximum becomes more complex, but essential for maximizing power output. An improved GMPP tracking method for PV systems under partial shading prioritizes power peaks closer to the open-circuit voltage (V_{OC}). This reduces the risk of overheating and hotspots, minimizes thermal stress, and enhances tracking speed by using the relationship between shaded cell temperature and the operating point [15]. Another study focuses on optimizing voltage search algorithms to efficiently find the GMPP by narrowing the search area and skipping unnecessary voltage ranges [16]. Additionally, an MPP scanning method is proposed, which utilizes a controlled voltage source to identify the GMPP under partial shading conditions, requiring minimal hardware and ensuring efficient operation [17]. A two-stage GMPP tracking algorithm based on an artificial neural network decreases tracking time and power losses by using fewer sampling points. This algorithm can be implemented without expensive sensors under complex partial shading conditions [18].

Considering the interconnection techniques of PV modules, some studies focus on array configuration which optimizes the fixed layout of PV modules, or array reconfiguration which dynamically adjusts connections to enhance performance under varying conditions [19, 20]. A modified fixed PV array configuration with reduced cross-ties is compared to Series (S), SP, total cross-tied (TCT), bridge-link (BL), and honey-comb (HC) configurations under various shading patterns. This configuration demonstrates lower mismatch losses, robust power generation, and reduced cabling compared to traditional TCT-based setups [21]. Several static PV array configurations under different shading patterns are studied using MATLAB/Simulink and real-time testing, and the performance of each is categorized according to environmental conditions [5]. A generalized panel rearrangement strategy is developed for irradiance mismatch conditions and system losses, optimizing module positions in TCT and SP configurations without extra sensors or switching circuits [6]. A modified PV arrangement and a progressive module shift rearrangement approach are introduced to emphasize efficient reconfiguration. This reduces wiring complexity and mismatch losses while enhancing power output under irradiance mismatch scenarios [22]. Additionally, a current injection-based dynamic array reconfiguration technique is proposed to improve PV array power output under partial shading. This method also eliminates multiple power-voltage peaks, reduces converter dependency, and simplifies MPPT requirements [23]. The performance of configurations may be improved by considering MPPT algorithms. One study presents a SP-cross-tied PV array configuration and evaluates its performance under various partial shading conditions. The study evaluates three different MPPT techniques and emphasizes the effectiveness of the fuzzy logic-based method in terms of tracking efficiency and faster settling times [24].

Module-level converters are another approach to mitigate the effects of partial shading [25–27]. A hybrid module-level power electronics system called the OptiVerter combines the features of microinverters and power optimizers. It utilizes a shade-tolerant MPPT algorithm and an ultra-wide input voltage range to harvest more energy and perform better under different shading conditions [25]. Another study introduces an integrated approach that combines a modified magic square-enhanced configuration, irradiance equalization, and SP differential power processing converters. This approach optimizes the power output of TCT-interconnected PV arrays, achieving significant power gains and high efficiency [26]. In [ref. 27], a module-level electronic circuit-based PV array reconfiguration approach enables automatic identification and decoupling of bypass modules under shading, reducing mismatch losses and improving energy efficiency without complex sensors.

In addition to conventional bypass diodes, new approaches have been developed to improve the performance of bypass diodes under partial shading conditions [28–32]. Overlapping bypass diodes in PV modules impact electrical performance, power losses, hotspot formation, and micro-inverter efficiency under partial shading, with a mathematical model revealing higher power dissipation and failure risks compared to non-overlapping configurations [28]. A MOSFET-based circuit is also proposed to optimize the performance of bypass diodes, reducing hotspot temperatures through a hotspot mitigation circuit [29]. Similarly, a self-activating bypass circuit is introduced, demonstrating its ability to eliminate power dissipation and temperature rise by interrupting the current flow in malfunctioning cells [30]. Another approach is to install a hotspot mitigation circuit, which prevents hotspots under mismatch conditions. This significantly reduces localized heating and power loss, while enhancing overall power output in both low and high shading scenarios [31]. An experimental study on the hotspot phenomenon is conducted to evaluate the effects of bypass diodes and TCT-configurations on thermal stress mitigation. The study revealed that, although TCT reduces mismatch losses, it fails to prevent hotspot formation, emphasizing the need for improved bypass mechanisms to enhance PV reliability. In addition, increasing the number of bypass diodes connected to each module is one of the important solutions developed at this point [33, 34]. However, the optimal bypass diode configuration and its impact on different PV array configurations remain an open research question.

This study aims to analyze how the number of bypass diodes affects PV array performance across different array configurations by using MATLAB/Simulink-Simscape. A detailed examination of GMPP behavior is conducted under 30 partial shading scenarios, considering variations in the number of cells per bypass diode (6, 12, 18,

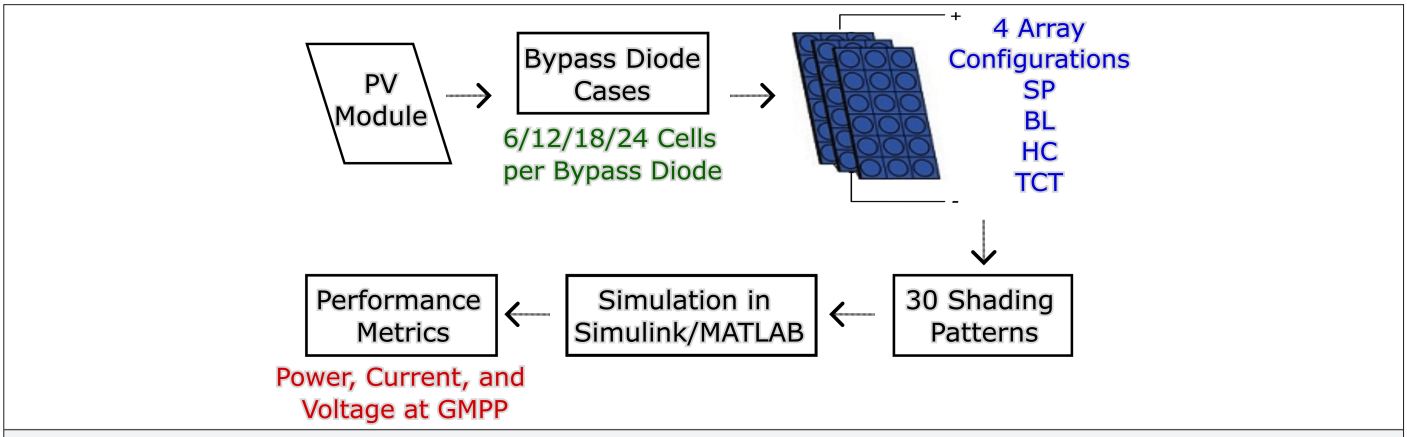

Fig. 1. Conceptual overview of the simulation framework utilized to evaluate the performance of PV arrays under partial shading conditions.

and 24). It provides an in-depth evaluation of bypass diode placement that influences PV system performance. The paper is organized as follows: section 2 presents the modeling of PV array configurations along with the bypass diode configurations. Shading scenarios employed in the analysis are given in section 3. In section 4, the GMPP values are presented for different scenarios, and the overall performance comparison is evaluated considering the number of bypass diodes and array configurations under partial shading. Finally, the conclusions of the study are presented in section 5.

II. MODELING AND SYSTEM CONFIGURATION

The subsequent sections outline the modeling approach to investigate how the quantity of bypass diodes influences various PV array configurations. Fig. 1 provides a concise overview of the simulation framework to enhance reader comprehension before detailing the modeling steps. This framework relies on a detailed cell-level analysis. The process begins with defining the PV module and its bypass diode configurations. By systematically altering the number of cells per bypass diode, the study aims to examine the changes in current, voltage, and power characteristics under randomly varying irradiance conditions. The performance of various PV array configurations, such as TCT, BL, HC, and SP, is evaluated for different numbers of cells per bypass diode under thirty distinct shading patterns. These setups are simulated in MATLAB/Simulink. To conduct a proper cell-level analysis, it is first essential to define the electrical characteristics of the PV module employed in the simulation. These parameters are critical for accurately capturing the array's operational behavior under varying bypass diode configurations.

A. Electrical Characteristics of Photovoltaic Module

The Simscape-Simulink model incorporates the single diode model shown in Fig. 2 which is known for its computational simplicity and accuracy. The equivalent circuit parameters are I_{PH} as photocurrent, R_S as series resistance, and R_P as parallel resistance. Model parameters are applicable for a cell or a module.

In this study, the PS-M72-405 PV module, consisting of 72 cells, is utilized. The electrical parameters of the module are provided in Table I for STCs (1000 W/m^2 irradiance and 25°C temperature), including open-circuit voltage (V_{OC}), short circuit current (I_{SC}), MPP voltage (V_{MPP}) and current (I_{MPP}), maximum power (P_{MAX}), and nominal operating cell temperature (NOCT). The single module data is obtained directly from the MATLAB Simulink device catalog and the module's datasheet [35].

After defining the electrical parameters of the PV module, the next step is to specify the bypass diode configurations, which determine how cells are connected and protected under partial shading. These configurations form the foundation for evaluating the system's response to different shading patterns.

B. Bypass Diode Cases

Bypass diode configurations are shown in Fig. 3. Each case assigns how many cells (e.g., 6, 12, 18, or 24) are connected per bypass diode. This means that in a 72-cell module, 12 bypass diodes are used for the 6-cell-per-diode case, 6 bypass diodes for the 12-cell case, 4 bypass diodes for the 18-cell case, and 3 bypass diodes for the 24-cell case. For each of the four bypass diode cases, 30 different irradiance

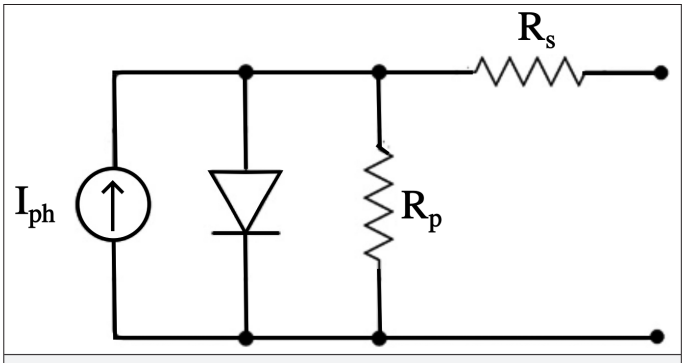

Fig. 2. Single diode equivalent circuit model of a PV cell.

TABLE I. ELECTRICAL PARAMETERS OF SINGLE PV MODULE UNDER STC (1000 W/M^2, 25°C).

Datasheet Parameters	
V_{OC}	50.32 V
I_{SC}	10.35 A
V_{MPP}	41.7 V
I_{MPP}	9.72 A
P_{MAX}	405 W
NOCT	45 ± 2°C

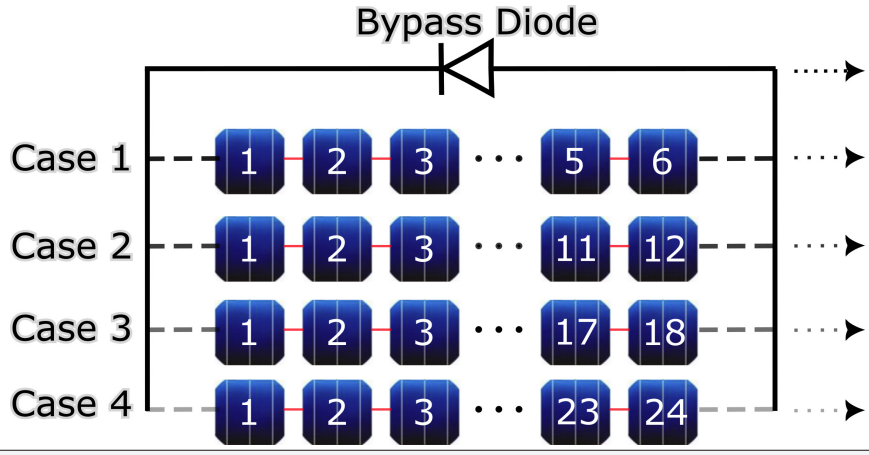

Fig. 3. Schematic representation of a single 72-cell PV module illustrating four different bypass diode configurations. Case 1: 6 cells per bypass diode (12 diodes), Case 2: 12 cells per diode (6 diodes), Case 3: 18 cells per diode (4 diodes), and Case 4: 24 cells per diode (3 diodes).

scenarios are simulated to evaluate their performance under varying shading conditions.

With the bypass diode cases established, the analysis proceeds to examine how various PV array configurations interact with these set-ups. The structural layout of the arrays is crucial in determining how effectively mismatch losses can be mitigated.

C. Photovoltaic Array Characteristics and Configurations

The PV arrays can be interconnected using various configurations to minimize mismatch losses and enhance energy efficiency. The most employed configurations in the literature are SP, TCT, BL, and HC. Each configuration offers distinct electrical characteristics and shading resilience, influencing the overall performance of the PV system under partial shading conditions [19, 20].

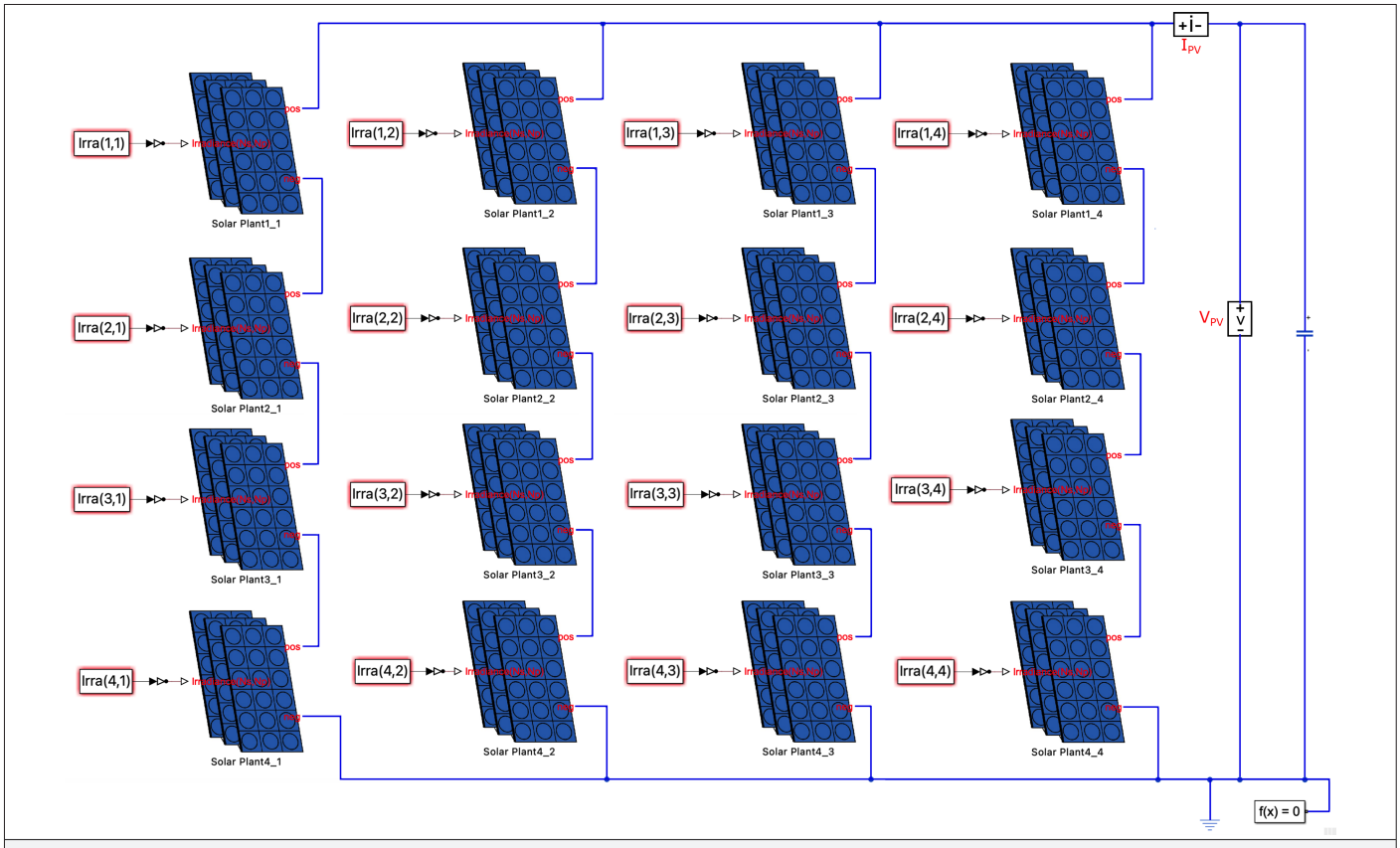

Fig. 4. MATLAB/Simulink-Simscape schematic of a PV array in a SP configuration. Each PV module is modeled with the Solar Plant block. Each "Irra(i,j)" input provides 12 irradiance values for the corresponding module, with values and ranges varying across modules based on the shading pattern.

In this study, these four PV array configurations are analyzed for different numbers of cells per bypass diode. The design of the 4 × 4 PV array is performed using MATLAB (Simulink-Simscape), with the schematic of the SP configuration shown in Fig. 4, BL in Fig. 5, HC in Fig. 6, and TCT in Fig. 7. In this context, the MATLAB solar plant model [36] is configured to represent a single module and to support varying irradiance levels for specific groups of cells. To ensure a consistent shading pattern, irradiance levels are assigned such that each of the six cells within a module receives the same irradiance. This procedure is implemented by considering the minimum number of cells per bypass diode. In addition, the model is also set up to accommodate different numbers of bypass diodes by adjusting the number of cells assigned to each diode, so that it can simulate module behavior under different bypass diode configurations. This approach allows for a detailed examination of the module and array performance, providing a cell-based analysis.

Simulations are assumed to be performed at a cell temperature of 45°C, which is equal to the nominal operating conditions. The GMPP voltages and currents of a 4 × 4 PV array are obtained for both 25°C and 45°C under uniform irradiance conditions (1000W/m^2) along with open-circuit voltage and short circuit current as shown in Table II. Those results will be considered as a reference because all array configurations yield exactly same results under uniform irradiance. As expected, increasing the temperature from 25°C to 45°C results in a slight increase in MPP current but a noticeable drop in MPP voltage. As a result, the maximum power (P_{MAX}) also decreases.

To summarize the modeling methodology discussed in this section, the key elements of the simulation setup are listed below:

- A single diode equivalent circuit is used to model the electrical behavior of the 72-cell PV module.
- Four bypass diode cases are defined by assigning 6, 12, 18, or 24 cells per diode.
- Simulink-Simscape environment is employed to simulate four array configurations: SP, TCT, BL, and HC.
- To represent more realistic field conditions, a cell temperature of 45°C under full irradiance (1000 W/m^2) is preferred over the standard 25°C reference.
- The modeling setup supports variable irradiance levels and flexible diode assignments for accurate analysis.

Once the array configurations and simulation parameters are defined, the next step is to apply realistic shading conditions to evaluate the performance of these configurations under nonuniform irradiance. The following section outlines the shading scenarios that are designed to facilitate this evaluation.

III. SHADING SCENARIOS

It is well known that environmental factors may lead to nonuniform irradiance distribution even across the module surface [37]. In addition, BIPV systems are frequently affected by fixed shading elements, which often result in intensive nonuniform irradiance characteristics [7]. Thus, the intensity of shading should be considered to evaluate

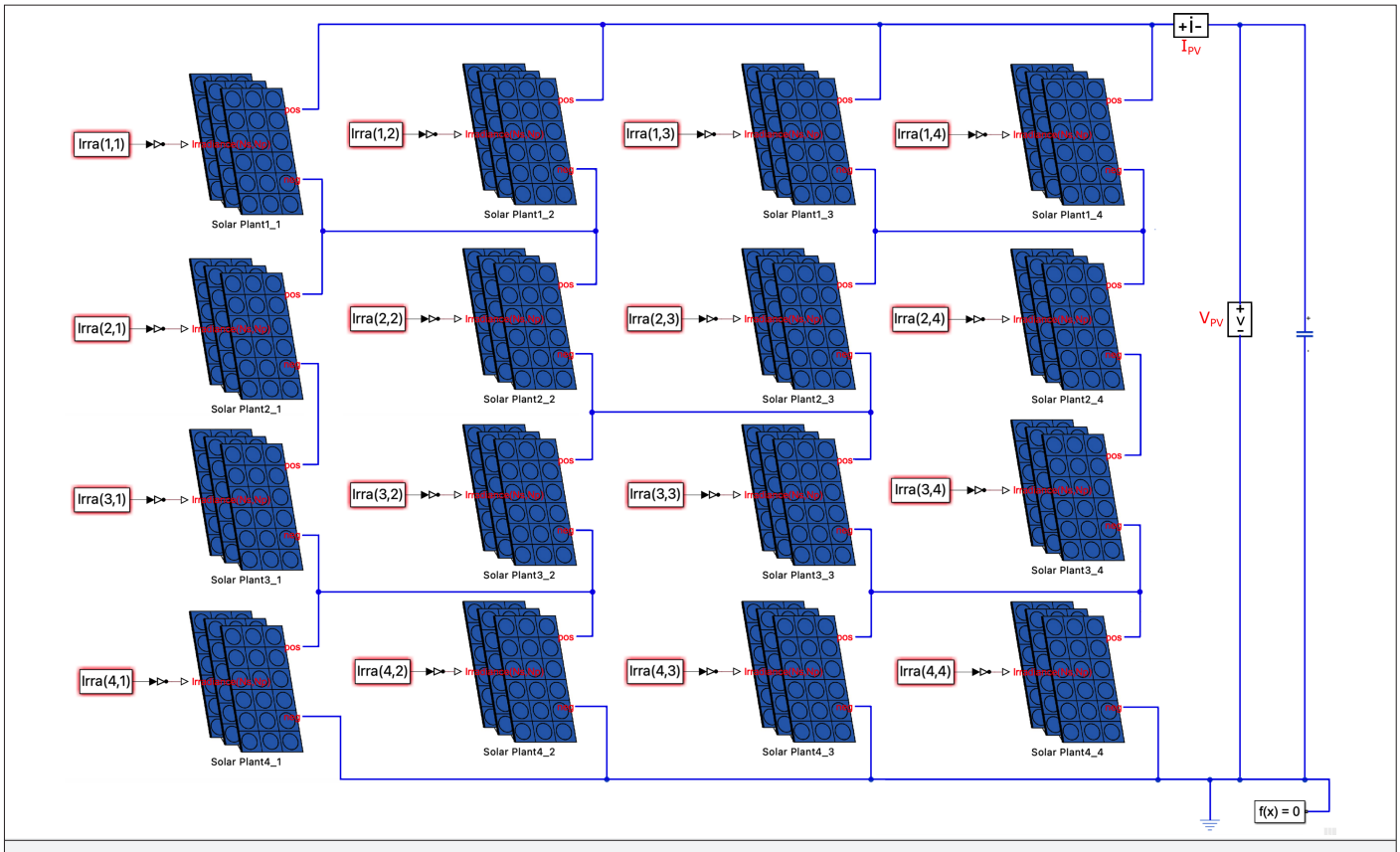

Fig. 5. MATLAB/Simulink-Simscape schematic of a PV array in a BL configuration. Each PV module is modeled with the Solar Plant block. Each "Irra(i,j)" input provides 12 irradiance values for the corresponding module, with values and ranges varying across modules based on the shading pattern.

the performance of array configurations under different bypass diode connection cases.

Several irradiance ranges are presented in Table III, each corresponding to a specific module, wherein groups of cells are subjected to randomly selected irradiance values within the defined range (in W/m^2). These ranges are categorized into variation levels (e.g., extreme, high, low), indicating the severity of nonuniformity across the module surface in each scenario. The ranges are considered in 30 different shading scenarios as shown in Fig. 8 to analyze the impact of nonuniform irradiance on PV array performance. Each of the 30 scenarios represents a 4 × 4 PV array configuration, where each individual box corresponds to a single PV module within the array. The numbers inside the modules denote different shading conditions based on the irradiance ranges specified in Table III, whereas white boxes represent unshaded areas with an irradiance of 1000 W/m^2. The irradiance values are randomly assigned within the specified range to simulate nonuniform shading conditions as mentioned before.

The shading scenarios applied include various patterns in which the shading intensity is distributed across the edges, corners, center, diagonally, or randomly across the array. Here, "Scenario 1" indicates the unshaded condition with an irradiance of 1000 W/m^2 and a cell temperature of 45°C. This scenario is designated as the reference case, serving as a baseline for comparison against partially shaded scenarios. The results corresponding to scenario 1 are given in Table II, showing identical values across all array configurations due to the absence of shading.

The modules are exposed to specific irradiance intervals across the 30 patterns. Each module is divided into six-cell segments, and each segment receives a distinct irradiance value within its assigned range. Patterns with broad intervals (e.g., 200–1000 W/m^2) simulate severe partial shading conditions, while patterns with narrower intervals (e.g., 700–1000 W/m^2) lead to low levels of irradiance nonuniformity. This systematic variation allows for a detailed assessment of array performance under different shading conditions.

Following the specification of irradiance distributions in the shading scenarios, simulations are consistently carried out for all cases of bypass diodes and array configurations. This ensures a fair and systematic performance evaluation. The next section presents and discusses the results, with particular emphasis on how the bypass diode quantity influences power, current, and voltage performance of PV arrays under partial shading conditions.

IV. ARRAY PERFORMANCE UNDER VARYING BYPASS DIODE CONFIGURATIONS

Performance of SP, BL, HC, and TCT-configurations under 30 partial shading scenarios is evaluated to observe the effect of shading and the number of bypass diodes on the overall power performance by analyzing the voltage, current, and power at GMPP. The power, current, and voltage values at GMPP are shown in Figs. 9-11, respectively. Scenario 1 in the figures represents the unshaded condition used as a reference.

Considering the power variations for all array configurations, scenarios with higher irradiance differences such as scenarios 8 and 30,

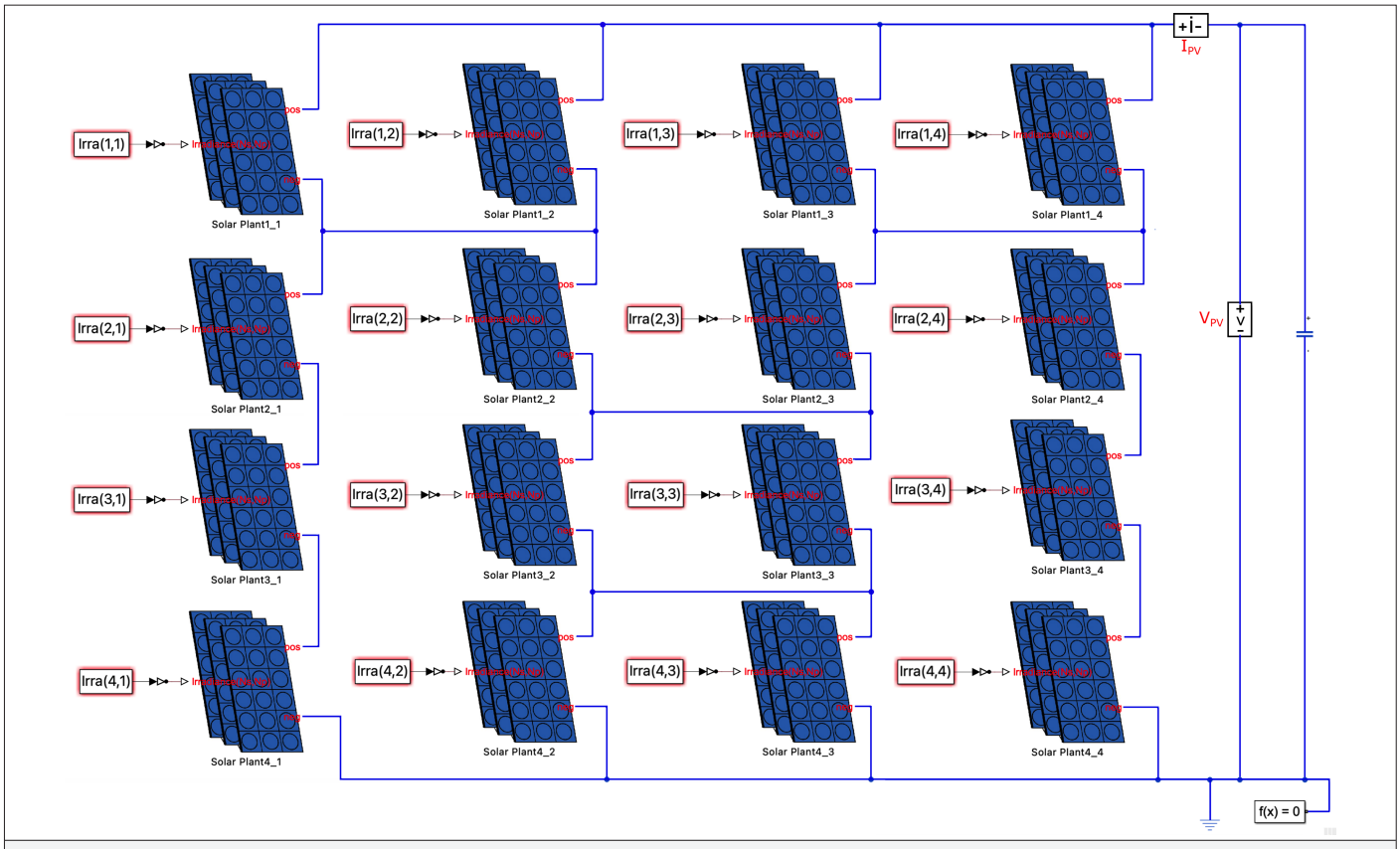

Fig. 6. MATLAB/Simulink-Simscape schematic of a PV array in a HC configuration. Each PV module is modeled with the Solar Plant block. Each "Irra(i,j)" input provides 12 irradiance values for the corresponding module, with values and ranges varying across modules based on the shading pattern.

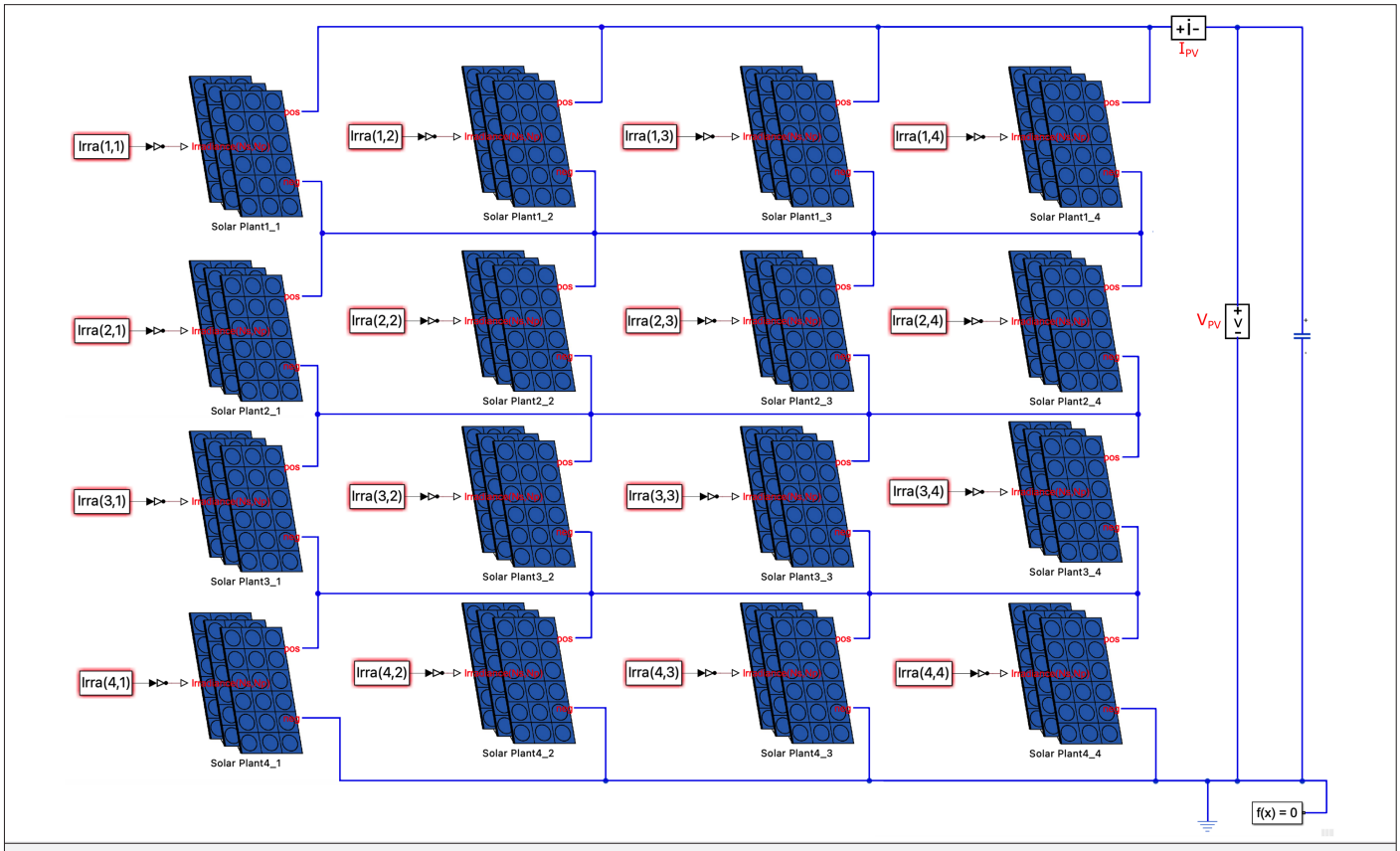

Fig. 7. MATLAB/Simulink-Simscape schematic of a PV array in a TCT-configuration. Each PV module is modeled with the Solar Plant block. Each "Irra(i,j)" input provides 12 irradiance values for the corresponding module, with values and ranges varying across modules based on the shading pattern.

which range from 200 to 1000 W/m^2 and involve shading over a large portion of the array, exhibit pronounced mismatch losses. These losses are particularly notable when a bypass diode is connected to more cells (e.g., 24 cells per bypass diode). Conversely, more bypass diode placement (e.g., 6 cells per bypass diode) mitigates the effects of partial shading, resulting in higher power in certain scenarios. It can be observed that there is a gradual decrease in GMPP power among the cases of 6, 12, 18, and 24 cells per bypass diode. While heavy shading results in greater power losses, increasing the number of bypass diodes improves performance in all configurations.

The array configurations with a higher number of cells per bypass diode reduce shading-induced mismatch losses at various levels. SP in Fig. 9(a) suffers the most from partial shading, experiencing sharp power losses, especially with fewer bypass diodes. BL in Fig. 9(b) provides an intermediate solution, mitigating shading effects better than SP. HC in Fig. 9(c) shows moderate shade resilience, but its hexagonal structure does not always outperform BL. TCT in Fig. 9(d) is the most robust configuration, showing minimal power loss under partial shading.

In terms of current, the currents of GMPP values have notable changes in all configurations as given in Fig. 10. Fig. 10(a) is for the SP configuration, Fig. 10(b) is for BL, Fig. 10(c) is for HC, and Fig. 10(d)

TABLE II. ELECTRICAL PARAMETERS OF PV ARRAY

	Irradiation and Temperature Conditions	
Parameters	**1000 W/m², 25°C**	**1000 W/m², 45°C**
V_{OC}	201.28 V	189.31 V
I_{SC}	41.4 A	41.9 A
V_{MPP}	166.8 V	154.54 V
I_{MPP}	38.88 A	38.92 A
P_{MAX}	6480 W	6014.8 W

TABLE III. IRRADIANCE RANGES OF SHADING SCENARIOS

Variation Level	Irradiation Ranges	Numbers
Extreme	200–1000W/m²	8, 11
Very high	300–1000W/m²	1, 4, 13
High	400–1000W/m²	5, 10
Moderate	500–1000W/m²	2
Mild	600–1000W/m²	3, 7
Low	700–1000W/m²	9
Very low	800–1000W/m²	6, 12

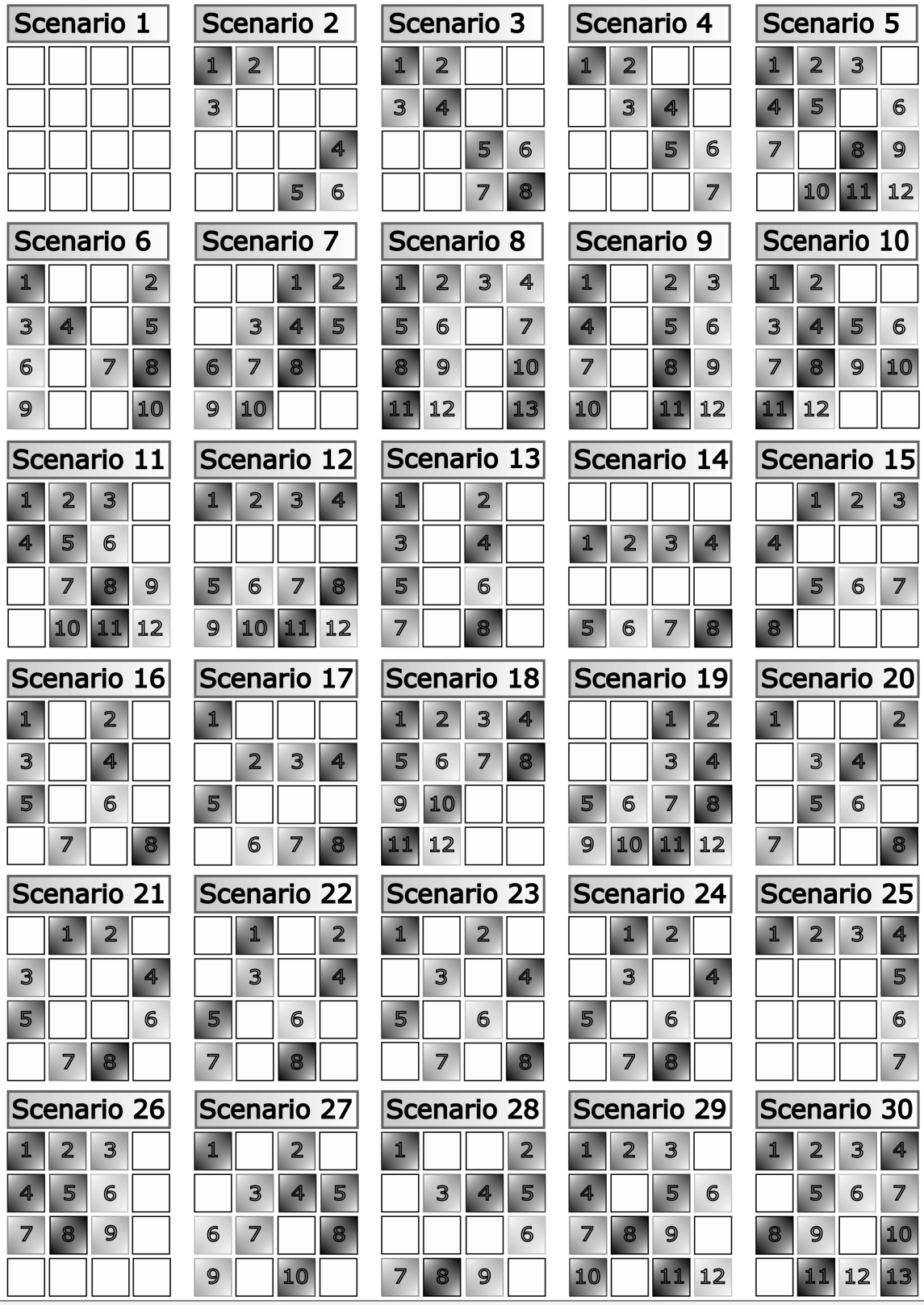

Fig. 8. Illustration of 30 partial shading scenarios across a 4 × 4 PV array. Each number refers to a specific irradiance range listed in Table III, while white modules receive full irradiance (1000 W/m^2).

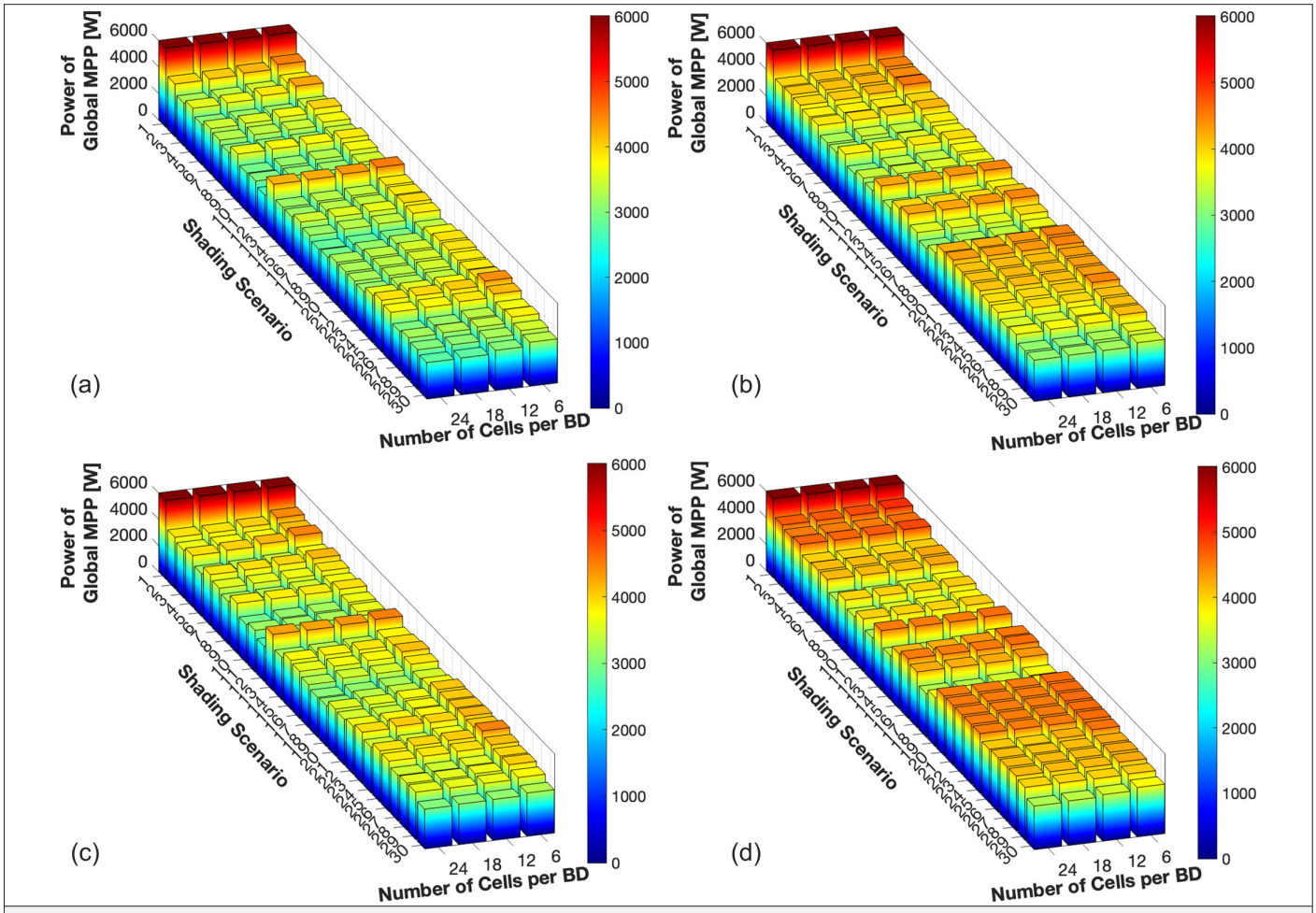

Fig. 9. GMPP power variation in (a) SP, (b) BL, (c) HC, and (d) TCT-configurations under different shading scenarios and number of cells per bypass diode (BD, bypass diode). Color scale from red to blue indicates high-to-low power levels.

is for TCT. Similar to the maximum power, current values show a clear decline with more pronounced reductions in cases where a higher number of modules are shaded (e.g., scenario 30). For scenarios with the same number of shaded modules, similar results are obtained depending on the configuration. This is particularly evident for scenarios 20–24 in the TCT-configuration, where the interconnection design ensures that rows with an equal number of shaded modules exhibit similar current values [38]. While increasing the number of cells per bypass diode generally results in a decreasing current trend, in some scenarios, fluctuations occur depending on the location and intensity of shading. This behavior is most pronounced in the SP, BL, and HC configurations, leading to larger deviations in global I_{MPP}. The TCT configuration demonstrates a more stable current profile, with minimal changes.

The voltage at GMPP values has larger voltage deviations under more severe shading conditions in comparison to the unshaded reference case. For the same shading scenario, different PV configurations do not exhibit similar voltage responses, indicating that the interaction between shading patterns, array configuration type, and bypass diode placement leads to distinct outcomes. For instance, in scenario 2, the SP configuration (Fig. 11(a)) shows a decrease as the number of cells per bypass diode increases, while the BL (Fig. 11(b)) and HC (Fig. 11(c)) configurations show an initial increase in voltage and then a decrease. In contrast, TCT in Fig. 11(d) provides relatively stable but slightly fluctuating voltage values. Similarly, in Scenario 30, SP shows an initial increase followed by a decrease in voltage with fewer bypass diodes, while TCT shows the opposite trend. These variations indicate the need to evaluate current and voltage behavior together to accurately interpret the performance of each array configuration. In some shading scenarios, voltage values exceed the unshaded case, indicating that the operating voltage shifts closer to the open-circuit voltage region due to a significant drop in current at GMPP. It is a direct consequence of the shift of GMPP toward a different voltage-current pair, indicating that the GMPP has moved. The presence of bypass diodes introduces multiple maxima in the P-V curve depending on the shading level [38, 39]. This causes the GMPP to shift as a function of irradiance levels. Under shading conditions, certain groups of cells are bypassed, altering the effective current paths and leading to MPP relocation along the voltage axis. While BL, HC, and SP exhibit moderate voltage variations across shading scenarios, TCT consistently demonstrates the highest stability in voltage values.

A more quantitative assessment is provided by Table IV, which shows the average values of the voltage, power, and current at GMPP across all the configurations. The table includes the average values of P_{MAX}, V_{MPP}, and I_{MPP} over the 30 partial shading scenarios considered. It

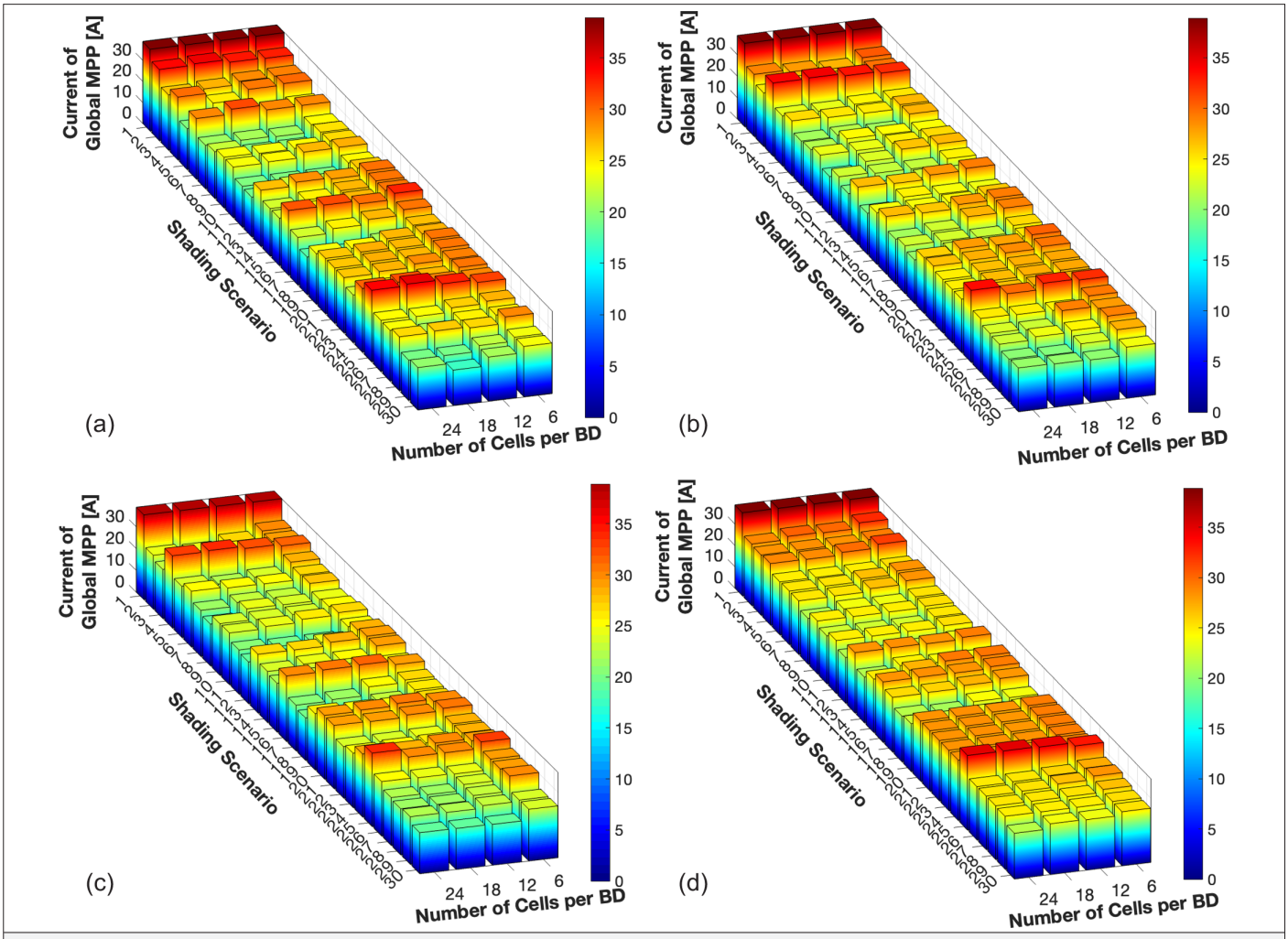

Fig. 10. GMPP current variation in (a) SP, (b) BL, (c) HC, and (d) TCT-configurations under different shading scenarios and number of cells per bypass diode (BD, bypass diode). Color scale from red to blue indicates high-to-low current levels.

allows a comparative analysis of the impact of configuration type and bypass diode placement on overall PV performance. Compared to the unshaded reference case in Table II (6014.8 W at 45°C), the average power obtained across all partial shading scenarios is significantly lower, often falling around 4000 W. This substantial decline is primarily due to the high shading intensity and nonuniform irradiance distribution. The above explanation is supported by the average GMPP results which a larger number of bypass diodes (i.e., 6 cells per bypass diode) consistently results in higher power output across all configurations. As the number of cells per bypass diode increases, a progressive decrease in P_{MAX} is observed. The SP exhibits the steepest decline, from 3904.1 W to 3368.6 W, followed by HC (4028.9 W to 3599.9 W) and BL (4133.9 W to 3790.6 W). The BL configuration exhibits a smaller percentage decrease in power output compared to the SP configuration, while the HC configuration follows a similar performance trend to that of BL. Among all configurations, TCT demonstrates the least power reduction, decreasing from 4326.9 W to 4146.2 W, thereby highlighting its superior adaptability under shading conditions. On the other hand, the current values of all configurations are notably lower than the reference case under uniform irradiance which is 38.92 A. When comparing the extremes—6 cells and 24 cells per bypass diodes—SP exhibits the largest current reduction with a difference of 3.231 A, followed by BL with 3.426 A, HC with 3.661 A, and TCT with the smallest decrease of 1.825 A. In conclusion, the results underscore the critical role of both array configuration and the number of bypass diodes in determining PV array performance under partial shading conditions. Among the evaluated configurations, TCT consistently achieves the highest performance in mitigating mismatch losses, primarily due to its inherent interconnection flexibility and its compatibility with increased bypass diode utilization. Increasing the number of bypass diodes effectively alleviates the adverse effects of shading by minimizing significant drops in the GMPP. In contrast, the series-connected nature of the SP configuration leads to current bottlenecks, where a single shaded module restricts the current flow of the entire string, thereby triggering frequent bypass diode activation. These findings highlight that the combination of an optimized bypass diode placement strategy and a robust array configuration, particularly the TCT topology, plays a vital role in enhancing PV system efficiency and energy yield under realistic operating conditions.

These findings collectively emphasize the critical role of bypass diode count in shaping array performance under nonuniform irradiance. Configurations employing a higher number of diodes

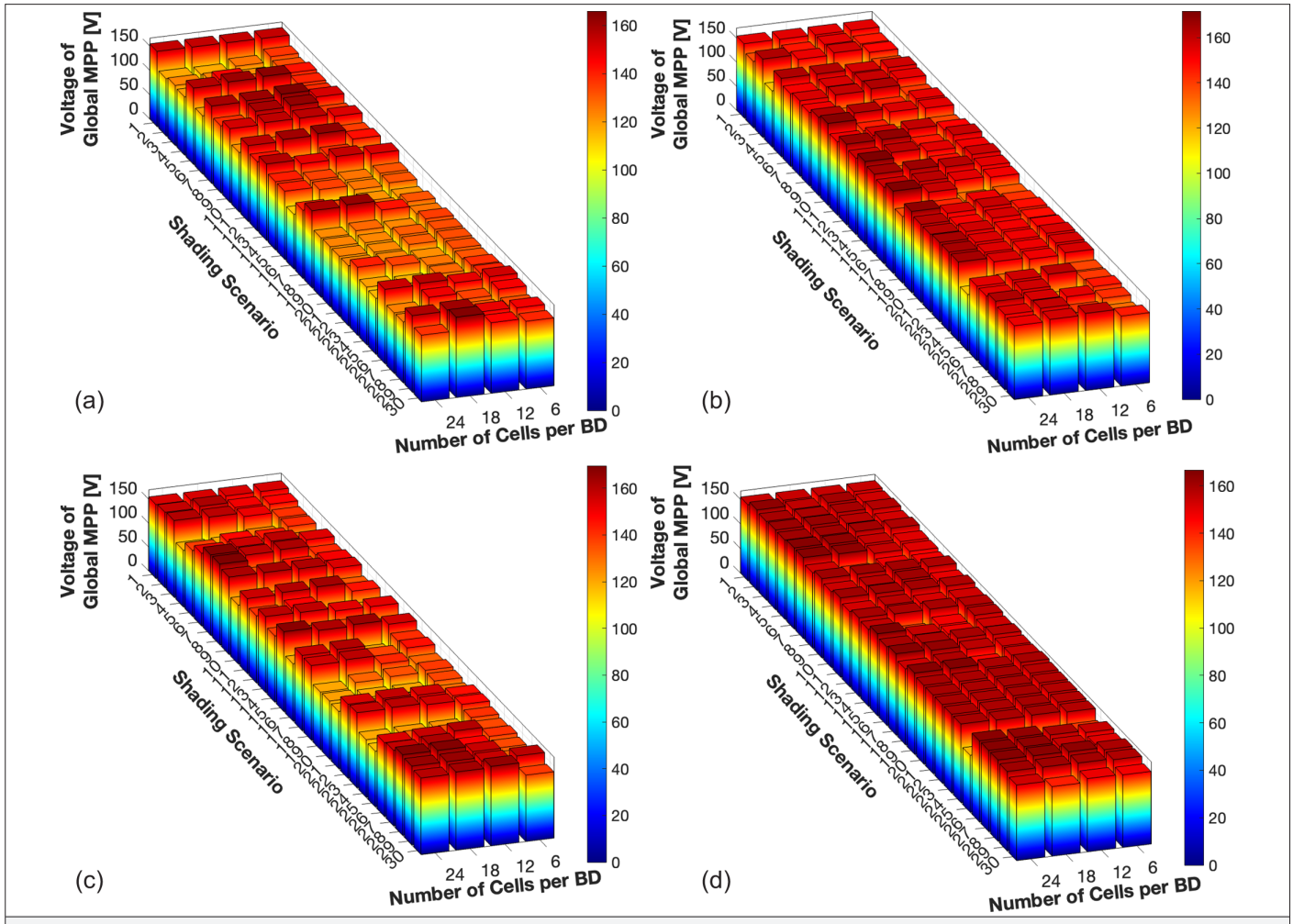

Fig. 11. GMPP voltage variation in (a) SP, (b) BL, (c) HC, and (d) TCT-configurations under different shading scenarios and number of cells per bypass diode (BD, bypass diode). Color scale from red to blue indicates high-to-low voltage levels.

consistently demonstrate improved power output and voltage stability due to reduced mismatch losses and more efficient current routing. By protecting smaller cell groups, more diodes reduce the reverse bias stress and allows for improved power extraction during irregular irradiance, contributing to higher long-term energy yields and operational stability [40]. This design choice also introduces specific manufacturing and operational trade-offs. Integrating more diodes requires additional interconnection points and soldering steps, which increases assembly complexity. This can lead to higher manufacturing costs due to the additional interconnections, precise soldering, and extended quality control required. In the long term, the higher number of contact points can increase the risk of thermal and mechanical degradation, which can lead to higher maintenance costs and shorter lifecycles [41, 42]. Furthermore, complex bypassing schemes can introduce multiple local maxima in the P-V curve, which can complicate MPPT operation [43].

Although including additional bypass diodes introduces manufacturing and operational challenges, the long-term performance advantages effectively offset these drawbacks. A greater number of diodes improves thermal protection by limiting reverse bias stress on shaded cells, thereby substantially reducing the risk of hotspot development [40]. This is a critical factor in long-term module degradation. Additionally, increased segmentation improves the resolution of voltage steps in the P-V curve, enabling more accurate GMPP tracking under variable shading conditions [33, 39]. These benefits support higher energy yield and operational stability, particularly in shade-prone environments [44]. Consequently, although the initial cost and design complexity may be higher, the long-term efficiency and durability gains have the potential to justify the investment, making these configurations especially advantageous for shade-prone PV applications.

V. CONCLUSION

Partial shading remains a major obstacle to maximizing the energy yield of PV systems, particularly in real-world environments where dynamic and nonuniform irradiance conditions are unavoidable. This study systematically investigated the impact of bypass diode configuration—specifically the number of cells per bypass diode—on the performance of four commonly used PV array configurations: SP, BL, HC, and TCT. Using a MATLAB Simscape model, 30 several partial shading scenarios are simulated to evaluate power, current, and voltage behavior at the GMPP.

TABLE IV. AVERAGE VALUES OF GMPP PARAMETERS FOR 30 PARTIAL SHADING SCENARIOS

Configuration	Cells per Bypass Diode	Average of P_{MAX} (W)	Average of V_{MPP} (V)	Average of I_{MPP} (A)
Series-parallel	6	3904.1	137.95	28.321
	12	3575.8	137.275	26.297
	18	3457.7	138.305	25.427
	24	3368.6	135.85	25.09
Bridge-link	6	4133.9	148.573	27.865
	12	3915.6	150.22	26.194
	18	3838.6	153.38	25.159
	24	3790.6	156.61	24.439
Honey-comb	6	4028.9	141.85	28.432
	12	3744.8	145.296	25.977
	18	3658.9	148.182	24.973
	24	3599.9	147.32	24.771
Total cross-tied	6	4326.9	154.663	27.999
	12	4200.6	155.714	27.022
	18	4156.8	156.67	26.61
	24	4146.2	158.853	26.174

The results reveal that both array and bypass diode configurations significantly influence the system's ability to mitigate mismatch losses. Increasing the number of bypass diodes consistently led to improved performance, particularly under severe shading conditions. Among the configurations, TCT demonstrates the highest robustness, maintaining relatively stable power output, current, and voltage levels across all scenarios. In contrast, the SP configuration suffers from the greatest performance degradation due to its sensitivity to series-connected current bottlenecks. While BL and HC offer intermediate resilience, their performance is still notably affected by the choice of bypass diode configuration.

Average performance metrics across all scenarios further confirm that more bypass diodes yield significant gains in GMPP power and current, regardless of array type. However, the degree of improvement is closely tied to the underlying interconnection strategy of each topology. These findings highlight the critical role of bypass diode design in optimizing PV system reliability and energy output. Future PV array designs, especially those for shaded or urban environments, may strategically integrate more bypass diodes in association with robust array configurations such as TCT to ensure superior mismatch handling and energy harvesting performance. Consequently, rather than making generalized comparisons between array configurations, it would be more appropriate to conduct site-specific evaluations that account for both the number of bypass diodes and the severity of partial shading condition.

Data Availability Statement: The data that support the findings of this study are available on request from the corresponding author.

Peer-review: Externally peer-reviewed.

Author Contributions: Concept – H.G.S.U.; Design – H.G.S.U.; Supervision – H.G.S.U.; Resources – H.G.S.U.; Materials – H.G.S.U.; Data Collection and/or Processing – H.G.S.U.; Analysis and/or Interpretation – H.G.S.U.; Literature Search – H.G.S.U.; Writing Manuscript – H.G.S.U.; Critical Review – H.G.S.U.

Declaration of Interests: The authors have no conflicts of interest to declare.

Funding: The authors declared that this study has received no financial support.

REFERENCES

1. S. P. Europe, "*Global Market Outlook for Solar Power 2024–2028*". Belgium: SolarPower Europe, 2024.
2. W. Xiao, *Photovoltaic Power System: Modeling, Design, and Control*. Chichester, UK: John Wiley & Sons, 2017. [CrossRef]
3. N. D. Kaushika, A. Mishra, and A. K. Rai, "*Solar Photovoltaics Technology, System Design, Reliability and Viability*". Berlin: Springer, 2018.
4. N. Kushwaha, V. K. Yadav, and R. Saha, "Effect of partial shading on photovoltaic systems performance and its mitigation techniques-a review," *Energy Sources A*, vol. 45, no. 4, pp. 11155–11180, 2023. [CrossRef]
5. S. Devakirubakaran, R. Verma, B. Chokkalingam, and L. Mihet-Popa, "Performance evaluation of static PV array configurations for mitigating mismatch losses," *IEEE Access*, vol. 11, pp. 47725–47749, 2023. [CrossRef]
6. R. Singh, V. K. Yadav, and M. Singh, "A comprehensive shade resilient approach for enhanced PV array performance under irradiance mismatch conditions," *IEEE J. Photovolt.*, vol. 14, No. 3, pp. 549–556, 2024. [CrossRef]
7. N. Martín-Chivelet et al., "Building-Integrated Photovoltaic (BIPV) products and systems: A review of energy-related behavior," *Energy Build.*, vol. 262, p. 111998, 2022. [CrossRef]
8. K. A. K. Niazi, Y. Yang, and D. Sera, "Review of mismatch mitigation techniques for PV modules," *IET Renew. Power Gener.*, vol. 13, no. 12, pp. 2035–2050, 2019. [CrossRef]
9. H. Abdulla, A. Sleptchenko, and A. Nayfeh, "Photovoltaic systems operation and maintenance: A review and future directions," *Renew. Sustain. Energy Rev.*, vol. 195, p. 114342, 2024. [CrossRef]
10. F. Belhachat, and C. Larbes, "Photovoltaic array reconfiguration strategies for mitigating partial shading effects: Recent advances and perspectives," *Energy Convers. Manag.*, vol. 313, p. 118547, 2024. [CrossRef]
11. M. Khodapanah, T. Ghanbari, E. Moshksar, and Z. Hosseini, "Partial shading detection and hotspot prediction in photovoltaic systems based on numerical differentiation and integration of the P–V curves," *IET Renew. Power Gener.*, vol. 17, no. 2, pp. 279–295, 2023. [CrossRef]
12. D. P. Winston, B. P. Kumar, S. C. Christabel, A. J. Chamkha, and R. Sathyamurthy, "Maximum power extraction in solar renewable power system-a bypass diode scanning approach," *Comput. Electr. Eng.*, vol. 70, pp. 122–136, 2018. [CrossRef]
13. M. Kermadi, V. J. Chin, S. Mekhilef, and Z. Salam, "A fast and accurate generalized analytical approach for PV arrays modeling under partial shading conditions," *Sol. Energy*, vol. 208, pp. 753–765, 2020. [CrossRef]
14. K. Lappalainen, and S. Valkealahti, "Photovoltaic mismatch losses caused by moving clouds," *Sol. Energy*, vol. 158, pp. 455–461, 2017. [CrossRef]
15. Z. Smara, A. Aissat, H. Deboucha, H. Rezk, and S. Mekhilef, "An enhanced global MPPT method to mitigate overheating in PV systems under partial shading conditions," *Renew. Energy*, vol. 234, p. 121187, 2024. [CrossRef]
16. Z. Sun, Y. Jang, and S. Bae, "Optimized voltage search algorithm for fast global maximum power point tracking in photovoltaic systems," *IEEE Trans. Sustain. Energy*, vol. 14, no. 1, pp. 423–441, 2023. [CrossRef]
17. B. Lin, L. Wang, and Q. Wu, "Maximum power point scanning for PV systems under various partial shading conditions," *IEEE Trans. Sustain. Energy*, vol. 11, no. 4, pp. 2556–2566, 2020. [CrossRef]
18. S. P. Ye, Y. H. Liu, H. Y. Pai, A. Sangwongwanich, and F. Blaabjerg, "A novel ANN-based GMPPT method for PV systems under complex partial shading conditions," *IEEE Trans. Sustain. Energy*, vol. 15, no. 1, pp. 328–338, 2024. [CrossRef]
19. F. Belhachat, and C. Larbes, "PV array reconfiguration techniques for maximum power optimization under partial shading conditions: A review," *Sol. Energy*, vol. 230, pp. 558–582, 2021. [CrossRef]

20. A. S. Yadav, and V. Mukherjee, "Conventional and advanced PV array configurations to extract maximum power under partial shading conditions: A review," *Renew. Energy*, vol. 178, pp. 977–1005, 2021. [CrossRef]
21. P. K. Bonthagorla, and S. Mikkili, "A novel fixed PV array configuration for harvesting maximum power from shaded modules by reducing the number of cross-ties," *IEEE J. Emerg. Sel. Top. Power Electron.*, vol. 9, no. 2, pp. 2109–2121, 2021. [CrossRef]
22. R. Singh, V. K. Yadav, and M. Singh, "Performance enhancement of a novel reduced cross-tied PV arrangement under irradiance mismatch scenarios," *Appl. Energy*, vol. 376, p. 124185, 2024. [CrossRef]
23. B. K. Karmakar, and G. Karmakar, "A current supported PV array reconfiguration technique to mitigate partial shading," *IEEE Trans. Sustain. Energy*, vol. 12, no. 2, pp. 1449–1460, 2021. [CrossRef]
24. D. K. Narne, T. A. Ramesh Kumar, and R. Alla, "Evaluation of series-parallel-cross-tied PV array configuration performance with maximum power point tracking techniques under partial shading conditions," *Clean Energy*, vol. 7, no. 3, pp. 620–634, 2023. [CrossRef]
25. D. Vinnikov, A. Chub, E. Liivik, R. Kosenko, and O. Korkh, "Solar optiverter—A novel hybrid approach to the photovoltaic module level power electronics," *IEEE Trans. Ind. Electron.*, vol. 66, no. 5, pp. 3869–3880, 2019. [CrossRef]
26. M. Etarhouni, B. Chong, and L. Zhang, "A combined scheme for maximising the output power of a Photovoltaic array under partial shading conditions," *Sustain. Energy Technol. Assess.*, vol. 50, p. 101878, 2022. [CrossRef]
27. A. F. Murtaza, H. A. Sher, K. Al-Haddad, and F. Spertino, "Module level electronic circuit based PV array for identification and reconfiguration of bypass modules," *IEEE Trans. Energy Convers.*, vol. 36, no. 1, pp. 380–389, 2021. [CrossRef]
28. Z. Alqaisi, and Y. Mahmoud, "Comprehensive study of partially shaded PV modules with overlapping diodes," *IEEE Access*, vol. 7, pp. 172665–172675, 2019. [CrossRef]
29. K. Baranwal, P. Prakash, and V. K. Yadav, "Optimizing bypass diode performance with modified hotspot mitigation circuit," *Sol. Energy Mater. Sol. Cells*, vol. 280, p. 113281, 2025. [CrossRef]
30. P. Guerriero, P. Tricoli, and S. Daliento, "A bypass circuit for avoiding the hot spot in PV modules," *Sol. Energy*, vol. 181, pp. 430–438, 2019. [CrossRef]
31. R. Singh, V. K. Yadav, and M. Singh, "An improved hot spot mitigation approach for photovoltaic modules under mismatch conditions," *IEEE Trans. Ind. Electron.*, vol. 71, no. 5, pp. 4840–4850, 2024. [CrossRef]
32. S. Ghosh, S. K. Singh, and V. K. Yadav, "Experimental investigation of hotspot phenomenon in PV arrays under mismatch conditions," *Sol. Energy*, vol. 253, pp. 219–230, 2023. [CrossRef]
33. M. Q. Duong, G. N. Sava, G. Ionescu, H. Necula, S. Leva, and M. Mussetta, "Optimal bypass diode configuration for PV arrays under shading influence," in Proc. of the 2017 IEEE Int. Conf. on Environment and Electrical Engineering and, 2017 IEEE Industrial and Commercial Power Systems Europe (EEEIC/I&CPS Europe), Milan, Italy, IEEEXplore, June 2017, pp. 1–5. [CrossRef]
34. IEA PVPS Task 13, "Performance of partially shaded PV generators operated by optimized power electronics," *Tech. Report IEA-PVPS T13-27:2024*, 2024
35. Philadelphia Solar, "Mono crystalline module," "PS-M 72–405 Datasheet"
36. MathWorks, "Analysis of solar photovoltaic system shading," *MATLAB Documentation* [Online]. Available: https://www.mathworks.com/help/sps/ug/solar-shading.html. .[Accessed: 18 March 2025]
37. J. G. Bessa, L. Micheli, F. Almonacid, and E. F. Fernández, "Monitoring photovoltaic soiling: assessment, challenges, and perspectives of current and potential strategies," *iScience*, vol. 24, no. 3, 102165, 2021. [CrossRef]
38. S. Malathy, and R. Ramaprabha, "Reconfiguration strategies to extract maximum power from photovoltaic array under partially shaded conditions," *Renew. Sustain. Energy Rev.*, vol. 81, pp. 2922–2934, 2018. [CrossRef]
39. S. Silvestre, A. Boronat, and A. Chouder, "Study of bypass diodes configuration on PV modules," *Appl. Energy*, vol. 86, no. 9, pp. 1632–1640, 2009. [CrossRef]
40. R. G. Vieira, F. M. de Araújo, M. Dhimish, and M. I. Guerra, "A comprehensive review on bypass diode application on photovoltaic modules," *Energies*, vol. 13, no. 10, p. 2472, 2020. [CrossRef]
41. E. J. Schneller et al., "Manufacturing metrology for c-Si module reliability and durability Part III: Module manufacturing," *Renew. Sustain. Energy Rev.*, vol. 59, pp. 992–1016, 2016. [CrossRef]
42. L. Koester, S. Lindig, A. Louwen, A. Astigarraga, G. Manzolini, and D. Moser, "Review of photovoltaic module degradation, field inspection techniques and techno-economic assessment," *Renew. Sustain. Energy Rev.*, vol. 165, p. 112616, 2022. [CrossRef]
43. S. K. Das, D. Verma, S. Nema, and R. K. Nema, "Shading mitigation techniques: State-of-the-art in photovoltaic applications," *Renew. Sustain. Energy Rev.*, vol. 78, pp. 369–390, 2017. [CrossRef]
44. N. A. Al-Rawi, M. M. Al-Kaisi, and D. J. Asfer, "Reliability of photovoltaic modules II. Interconnection and bypass diodes effects," *Sol. Energy Mater. Sol. Cells*, vol. 31, no. 4, pp. 469–480, 1994. [CrossRef]

Hatice Gül Sezgin-Ugranlı, received her B.Sc. and M.Sc. degrees in Electrical and Electronics Engineering from Istanbul University, Turkey, in 2010 and 2014, respectively. She received her Ph.D. from Istanbul University-Cerrahpasa in 2020. She is currently an Assistant Professor in the Department of Electrical and Electronics Engineering at Izmir Bakircay University, Turkey. Her research interests include photovoltaic systems, semiconductor devices, semiconductor device reliability, and electronic circuits.